How to cite: *Angew. Chem. Int. Ed.* **2023**, e202310274
doi.org/10.1002/anie.202310274

Photochemistry **Hot Paper**

The Power of Action Plots: Unveiling Reaction Selectivity of Light-Stabilized Dynamic Covalent Chemistry

Steven C. Gauci, Filip E. Du Prez, Joshua O. Holloway, Hannes A. Houck, and Christopher Barner-Kowollik**

Abstract: Exploiting the optimum wavelength of reactivity for efficient photochemical reactions has been well-established based on the development of photochemical action plots. We herein demonstrate the power of such action plots by a remarkable example of the wavelength-resolved photochemistry of two triazolinedione (TAD) substrates, i.e., aliphatic and aromatic substituted, that exhibit near identical absorption spectra yet possess vastly disparate photoreactivity. We present our findings in carefully recorded action plots, from which reaction selectivity is identified. The profound difference in photoreactivity is exploited by designing a 'hybrid' bisfunctional TAD molecule, enabling the formation of a dual-gated reaction manifold that demonstrates the exceptional and site-selective (photo)chemical behavior of both TAD substrates within a single small molecule.

[*] S. C. Gauci, Dr. J. O. Holloway, Prof. C. Barner-Kowollik
School of Chemistry and Physics, Queensland University of Technology (QUT), 2 George Street,
QLD 4000 Brisbane (Australia)
and
Centre for Materials Science,
Queensland University of Technology (QUT), 2 George Street
QLD 4000 Brisbane (Australia)
E-mail: christopher.barnerkowollik@qut.edu.au

Prof. F. E. Du Prez
Department of Organic and Macromolecular Chemistry, Ghent University, Campus Sterre
Krijgslaan 281 S4-bis, 9000 Ghent (Belgium)

Dr. H. A. Houck
Department of Chemistry and Institute of Advanced Study, University of Warwick
Library Road, Coventry, CV4 7AL (UK)
E-mail: Hannes.Houck@warwick.ac.uk

Prof. C. Barner-Kowollik
Institute of Nanotechnology, Karlsruhe Institute of Technology (KIT)
Hermann-von-Helmholtz-Platz 1, 76344 Eggenstein-Leopoldshafen (Germany)

Introduction

The precise control of chemical reactivity constitutes the foundation of key biological and chemical processes.[1] Mimicking these processes synthetically, however, is considered a grand challenge and one that chemists have endeavored to overcome for decades.[2] In order to realize this vision, it is critical to apply external stimuli that address reactivity in a selective and/or orthogonal manner.[3] One appealing option to enable precise control over chemical transformations is the use of light.[4] Light-gated reactions are typically non-invasive, offer high spatiotemporal and energy precision, and can be performed at ambient temperatures.[5] In addition, an unparalleled level of reaction control can be achieved by altering the irradiation wavelength and/or intensity.[6] For example, the Hecht team has explored the incorporation of molecular photoswitches into photochromic systems, enabling the on-demand modulation of material properties upon exposure to specific wavelengths of light.[7] Similarly, photoswitches have been embedded into catalytically proficient molecules, whereby reversible changes induced by light can be translated into distinct alterations in catalytic function.[8] Furthermore, light has been used as fuel to drive translational and rotary motion in molecular machines, thereby enabling precise control over nanoscale movements and functions.[9] Such a remarkable level of reaction control highlights the transformative potential of light in manipulating chemical systems.

While absorption spectra are traditionally used to determine the most efficient irradiation wavelength for photoactivation, they have recently been demonstrated to be unreliable in predicting the actual wavelength-dependent reactivity of a photoreactive chromophore.[10] Indeed, the photochemical reactivity can depend strongly on the substitution pattern of the chromophore in question (e.g., aliphatic vs aromatic), despite having a similar absorption profile.[11] This was recently highlighted for aliphatic maleimides that undergo much more efficient cross [2+2] cycloadditions with alkenes compared to their aromatic substituted counterparts.[12] Over the last decade, our group has shown—using so-called photochemical 'action plots'—that the wavelength-dependent reactivity maximum is often red-shifted relative to the absorption maximum.[13] In other words, irradiating a chromophore at its maximum wavelength of absorption will in most cases not result in conducting a photochemical process with the highest

possible efficiency. Therefore, it is necessary to investigate the conversion of a photochemical process at a range of monochromatic wavelengths to identify the most efficient irradiation conditions. Thus, an action plot analysis employs a wavelength-tunable laser setup to induce a photochemical reaction at specific wavelengths with an identical photon count for each of the investigated wavelengths. Consequently, an action plot is obtained by mapping the reaction conversion as a function of wavelength, which provides better photoreactive insights compared to absorption spectra. We refer the interested reader to a detailed 'How-To' in the Supporting Information section of our recent overview of photochemical action plots.[10] Additionally, Turro and Lamola's previous work provides a list of specific conditions required to obtain biological 'action spectra'.[14] Obtaining such precise photochemical reactivity maps has been demonstrated to be important towards designing λ-orthogonal systems with the purpose of, for example, generating spatially resolved materials and 3D printing inks.[15]

In 2019, a collaborative effort between our teams' resulted in the design of a new type of photoresponsive covalent networks referred to as 'light-stabilized dynamic materials' (LSDMs).[16] The underpinning crosslinking chemistry in LSDMs is driven by an out-of-equilibrium photocycloaddition reaction between triazolinedione (TAD) and naphthalene that is, and remains, completely shifted to the adduct side during visible light irradiation.[17] The formed adducts remain stable while continuously irradiated but spontaneously dissociate once 'subjected' to darkness, resulting in de-crosslinking and liquification of the polymer network.[18]

In order to fully exploit the powerful photoreactivity of TAD moieties,[19] it is imperative to quantitatively map its wavelength-dependent reactivity. We herein identified—via a detailed action plot analysis—that two differently R-substituted TAD substrates i.e., an aliphatic (**1**) and aromatic (**3**), have very different photochemical reactivity towards naphthalene (**2**) cycloaddition, despite having a similar absorption profile (Scheme 1a–b). Specifically, we demonstrate that the photoreactivity is shifted relative to the TAD absorption spectrum and thus does not directly correlate to the compound's light absorption. Most importantly, we demonstrate that in the visible region of the n→π* transition, **1** is photochemically reactive towards naphthalene, while **3** shows close to no photochemical reactivity in the presence of naphthalene (Scheme 1c). Subsequently, an action plot analysis is employed to establish a site-selective reaction system, exploiting the powerful ligation characteristics of the TADs within a single molecule (Scheme 1d).

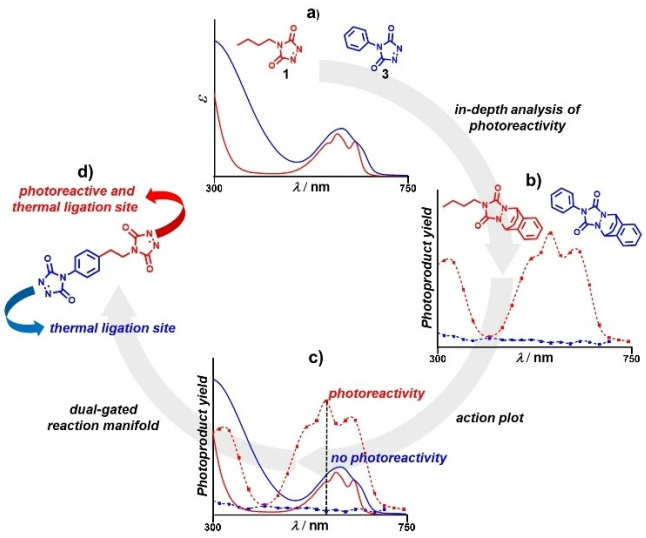

Scheme 1. Overview of the present study. (a-b) An in-depth action plot analysis on two 4-substituted TAD substrates—that exhibit very similar absorption spectra—reveals that one is photochemically reactive while the other shows close to no photoreactivity with naphthalene. (c-d) Subsequently, their difference in photoreactivity is exploited by introducing a hybrid-bisTAD molecule allowing for the design of a dual-gated reaction manifold, resulting in site-specific ligation reactivity.

Results and Discussion

Initially, a series of time-lapse irradiation experiments were carried out in order to elucidate the optimal parameters to obtain the action plot (i.e., number of photons) of the light-stabilized dynamic TAD-naphthalene cycloaddition. Since the TAD-naphthalene conjugation is known to proceed efficiently with aliphatic TADs under green-light irradiation,[20] a pink solution of 4-*n*-butyl-TAD (**1**, 15 mM in deuterated chloroform, $CDCl_3$) in the presence of naphthalene (**2**, 1.2 molar equivalent relative to **1**) was irradiated with monochromatic laser light ($\lambda_{max}=525$ nm, 500 μJ) to monitor the formation of the TAD-naphthalene photoproduct (**1a**) (Figure 1a, refer to Section 3.1 and 3.2, Supporting Information). After 70 min of irradiation at room temperature, the characteristic pink color completely disappeared, whereby the exclusive conversion of **1** into **1a** was confirmed by ^{1}H NMR spectroscopy (Figure S4–5, Supporting Information). Time-dependent monitoring of the cycloadduct formation indicated that 35 % of **1a** is formed after 15 min (Figure S5). Therefore, this time point was used to determine the number of photons for the action plot analysis, aligning with the recommended target of approximately 30 % photoproduct conversion.[10] In order to keep the number of incident photons constant during the action plot analysis, the laser energies and irradiation time have been adjusted across all wavelengths accordingly, also taking into account the wavelength-dependent transmittance of the glass laser vials (Figure S2).[10]

Having identified a suitable number of incident photons to conduct the action plot analysis, **1** (15 mM in $CDCl_3$) in the presence of **2** (1.2 molar equivalent relative to **1**) was irradiated with monochromatic laser light from $\lambda=300$ up to $\lambda=750$ nm in 15 nm wavelength increments (with a constant 34 μmol of photons, Figure 1a). The conversion of **1** into **1a** was confirmed by ^{1}H NMR spectroscopy before and after irradiation (Figure 1b). For this, the integral of the ^{1}H resonance at $\delta=3.66$ ppm for **1** (proton d), and $\delta=3.39$ ppm for **1a** (proton d') was used to quantify the conversion of **1** into **1a**.

In contrast to aliphatic substituted TADs, their aromatic analogues have been reported occasionally to undergo far

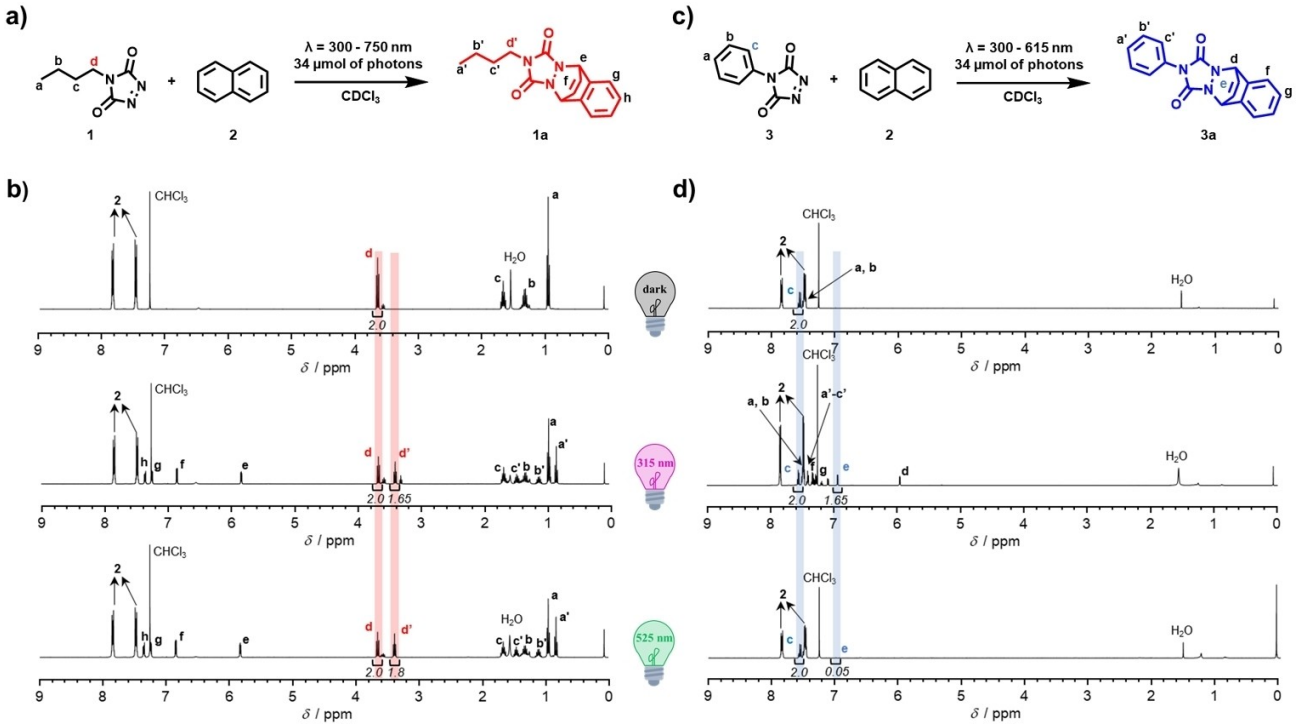

Figure 1. Light-stabilized dynamic TAD-naphthalene cycloaddition. (a) 4-*n*-butyl-TAD (**1**, 15 mM in $CDCl_3$) in the presence of naphthalene (**2**, 1.2 molar equivalent relative to **1**) subjected to monochromatic laser light (λ = 300–750 nm, 34 µmol of photons), resulting in the formation of photoproduct **1a**. (b) The formation of **1a** evidenced by ^{1}H NMR spectroscopy before (top) and after laser irradiation at λ_{max} = 315 and 525 nm (center and bottom, respectively). (c) 4-phenyl-TAD (**3**, 15 mM in $CDCl_3$) in the presence of naphthalene (**2**, 1.2 molar equivalent relative to **3**) subjected to monochromatic laser light (λ = 300–615 nm, 34 µmol of photons), resulting in the formation of photoproduct **3a**. (d) The formation of **3a** evidenced by ^{1}H NMR spectroscopy before (top) and after laser irradiation at λ_{max} = 315 and 525 nm (center and bottom, respectively).

less efficient photochemical transformations.[21] Thus, following the in-depth photoreactivity screening of the naphthalene cycloaddition with an aliphatic 4-substituted TAD, the wavelength-dependent reactivity of 4-phenyl-TAD (**3**, 15 mM in $CDCl_3$) in the presence of **2** (1.2 molar equivalent relative to **3**) was probed (Figure 1c). Following monochromatic laser light irradiation (λ = 300–615 nm, 15 nm increments, 34 µmol of photons), ^{1}H NMR spectroscopy was used before and after irradiation to confirm the formation of **3a**, whereby the integral of the ^{1}H resonance at δ = 7.56 ppm for **3** (proton c), and δ = 6.94 ppm for **3a** (proton e) was used to quantify the conversion of **3** into **3a** (Figure 1d). For the detailed synthetic and experimental procedures to determine the wavelength dependent conversion, we refer to section 3.3, Supporting Information.

The action plots for **1a** and **3a** formation reveal remarkable differences in the photochemical reactivity of the aliphatic and aromatic TAD substrates, despite having similar absorption properties (Figure 2, with red and blue squares, left *y*-axis, and solid red and blue line, right *y*-axis, respectively). For **1**, a broad absorbance band can be observed in the visible region between 480 and 580 nm. However, the action plot indicates an extended wavelength regime at which photoreactivity occurs ranging from 450 up to 615 nm. Indeed, whereas a local visible light absorption minimum occurs at 528 and 559 nm, the reactivity minimum is shifted to 510 and 540 nm (39 % and 38 % conversion,

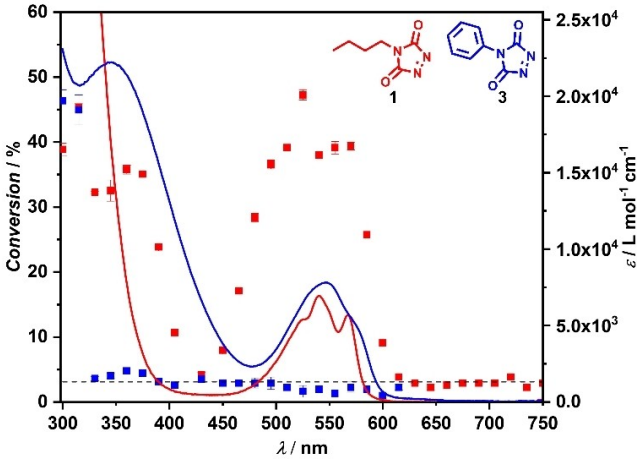

Figure 2. Wavelength-dependent reactivity (action plot) of substrates **1** (red squares) and **3** (blue squares) after irradiation with 34 µmol of photons at each wavelength, overlaid with the thermal reactivity of the substrate **1** (dash black line), and molar extinction coefficients of **1** (solid red line) and **3** (solid blue line). All measurements were carried out in triplicates and the error bars indicate the standard deviation of the data.

respectively). While the absorption maximum is observed at 541 nm, the maximum reaction yield is significantly blue-

shifted to 525 nm, reaching 47 % conversion into **1a** (Figure 2).

Toward shorter wavelengths, the absorption spectrum of **1** shows a broad and intense $\pi\rightarrow\pi^*$ transition, in which, two reaction yield maxima are observed (i.e., 45 % and 36 % at 315 and 360 nm, respectively), that are red-shifted compared to the UV-absorption band. In fact, reactivity is significantly red-shifted up to 405 nm throughout the UV absorbance band. Notably, **1a** cycloadduct formation with the aliphatic TAD proceeds with apparent higher efficiency under visible light activation relative to UV light, despite the much lower molar absorption coefficient. Given that certain cycloadducts can be photochemically reversed to their initial species with shorter wavelengths, and therefore could contribute to lower conversions in the UV-regime, we investigated the potential cycloreversion of **1a** under 315 nm irradiation. Thus, a pink solution of **1** (15 mM, $CDCl_3$) and **2** was first subjected to 525 nm for 1 h, to afford a colorless solution of **1a**, with >97 % conversion (Figure S18a). Subsequently, the colorless solution containing **1a** was irradiated with 315 nm laser light for 1 h, resulting in no change in color or conversion (i.e., remaining **1a** >97 %, Figure S18b). In contrast, a reference solution of **1a** (formed only by 525 nm irradiation) regained a faint pink color upon standing in the dark for 1 h, indicating the regeneration of **1**. In addition, a decrease in the conversion of **1a** from 97 to 87 % was observed in the ^{1}H NMR spectrum (Figure S18c). Thus, no net photocycloreversion occurs during 315 nm irradiation, and therefore does not account for the lower TAD/naphthalene photoreactivity observed in the UV-regime of the action plot. Further, it should be noted that some thermal background reactivity at room temperature can be observed for the TAD/naphthalene system. Hence, in a control experiment, a solution of **1** (15 mM, in $CDCl_3$) and **2** (1.2 molar equivalent relative to **1**) was prepared and kept at room temperature completely shielded from any light for 8 h. As confirmed via ^{1}H NMR spectroscopy, **1a** was indeed formed via a thermally driven process, albeit in trace amounts (3 %, Figure 2, dash black line). Importantly, an equilibrium is reached, and the conversion does not change after an additional 24 h dark period (refer to Figure S19, Supporting Information). Thus, although a 4 % conversion is obtained upon 430 nm irradiation, photoreactivity at this wavelength can be dismissed since a similar conversion is obtained thermally.

The photoreactivity of the aromatic TAD substrate **3** is remarkably different in comparison to its aliphatic counterpart (Figure 2, blue squares, left *y*-axis, and solid blue line, right *y*-axis). Indeed, whereas significant yield of the corresponding TAD-naphthalene cycloadduct was obtained between 450 and 615 nm, only trace amounts of **3a** are formed throughout this region (up to 3 %). Meanwhile, the yield of **3a** does not exceed 5 % between 330 and 480 nm, despite the strong absorption properties of **3** in this region. However, there is significant **3a** formation at 300 nm (46 %) and 315 nm (45 %), which is blue-shifted compared to the corresponding absorption band. In addition, no thermal cycloadduct is formed when a stock solution of **3** and **2** in $CDCl_3$ is kept in the dark for 24 h (Figure S20, Supporting Information).

With two detailed action plots at hand, we proceeded to exploit the profound difference in photoreactivity between substrates **1** and **3** in the presence of naphthalene in the visible light regime. To this end, a novel bisfunctional-hybrid-TAD molecule (**6**) was designed and synthesized, fusing both an aliphatic and aromatic TAD moiety in one molecule (Figure 3a, also refer to section 3.4 for the detailed synthetic procedure, Supporting Information). Specifically, the two disparate TAD moieties (i.e., **1** and **3**) have been combined into a single molecule for the design of a dual-gated reaction manifold in which light-induced naphthalene cycloaddition can be exclusively directed onto the aliphatic TAD site. Indeed, subjecting a dark red solution of **6** (15 mM in deuterated acetonitrile, CD_3CN) and **2** (1.2 molar equivalent relative to **6**) to green light irradiation for 3 h (λ_{max} = 525 nm, 2×10 W, refer to Figure S28), resulted in the exclusive formation of photoproduct **6a** with >95 % conversion as confirmed by NMR spectroscopy (Figure 3b, also refer to Figure S29–31). A color change from red into a less intensely colored pink solution was observed, owing to the unreacted aromatic TAD entity (Figure S32). Since no cycloadduct formation was observed when a reference mixture of **6** and **2** is placed in the dark at 80 °C for 3 h (^{1}H NMR spectrum, Figure S33), any temperature increase during laser irradiation is unlikely to promote the cycloaddition yield. Subsequently, the less intense pink solution of **6a** was placed in the dark at 25 °C and the cycloreversion was monitored over 17 h by ^{1}H NMR spectroscopy (refer to Table S1 and Figure S34, Supporting Information). Over the course of this 17 h dark period, the original intense red color returned, which is attributed to the release of **2** and the near-quantitative regeneration of **6** (>95 %), with an observed half-life of 4 h. The site-selective photocycloaddition thus allows for the selective transformation of the aliphatic TAD end of **6** into a latent functionality while retaining the reactivity of the aromatic end. Interestingly, continued irradiation of **6a** with 315 nm in the presence of excess naphthalene (i.e., 2.2 eq.) in CD_3CN did not yield additional cycloadduct formation onto the aromatic TAD end. However, upon repeating this experiment in 20:1 vol % $CDCl_3$:CD_3CN—whereby the small amount of acetonitrile was needed to ensure **6** was completely solubilized—the aromatic TAD end of **6a** (pre-formed after 3 h green light irradiation) was also transformed successfully into the corresponding photocycloadduct using UV laser light (λ = 315 nm, 65 % conversion after 90 min, refer to Section 3.5.3, Supporting Information). After placing the resulting mixture containing the double-end capped photocycloadduct in the dark for 24 h at room temperature, 93 % of **6** was regenerated (Figure S36). The latent functionality that is regenerated via the spontaneous cycloreversion at room temperature, thus provides a light-regulated protecting group strategy for reactive triazolinedione compounds, which can even differentiate between aromatic and aliphatic-based TAD protection based on solvent choice.

The hybrid compound **6** introduces a unique visible light-gated control over TAD reactivity that can be rever-

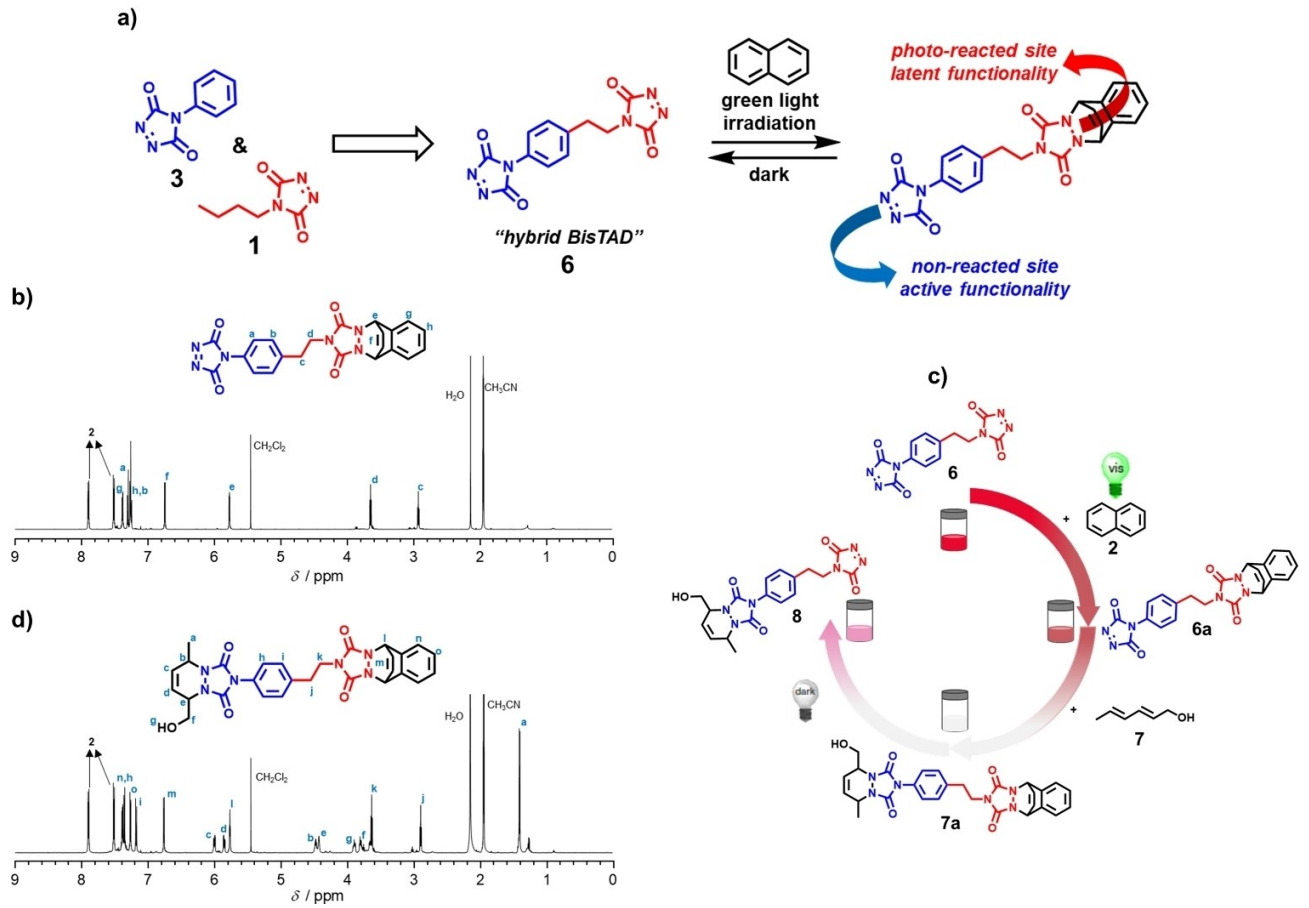

Figure 3. Dual-gated TAD reaction manifold. (a) A novel 'hybrid bisTAD' (**6**), which was designed and synthesized by combining both an aliphatic (**1**) and aromatic (**3**) TAD moiety into a single molecule. Subjecting a solution of **6** and naphthalene to green light irradiation allows for the site-selective photocycloaddition, which transforms the aliphatic end of **6** into a latent functionality while retaining the reactivity of the aromatic end. When placed in the dark, however, the latent functionality is regenerated via a spontaneous cycloreversion at room temperature, thus providing a promising protecting group strategy for TADs. (b) The exclusive formation of photoproduct **6a** with $>95\,\%$ conversion evidenced by ^{1}H NMR spectroscopy. (c) Small molecule ligations to demonstrate the dual-gated TAD reaction manifold. Initially, an intense red solution of **6** (15 mM in CD_3CN) and **2** (1.2 molar equivalent relative to **6**) is subjected to visible light to exclusively form a pink solution of photoproduct **6a**. Subsequently, the addition of **7** in the presence of **6a** gives the 1:1 Diels–Alder adduct **7a**, readily resulting in a colorless solution. Finally, the colorless solution is shielded from the light for 24 h to form **8**, resulting in the characteristic pink TAD color to return. (d) The conversion of **6a** into **7a** confirmed by ^{1}H NMR spectroscopy.

sibly toggled between a bis- and mono-functional reagent by switching green light on/off. To further exemplify the selective photoreactivity of **6**, a dual-reaction manifold was devised by combining the naphthalene photocycloaddition with the room temperature conjugation of TADs with olefinic substrates.[22] As depicted in Figure 3c, small molecule ligations were conducted to demonstrate this dual-gated reaction manifold (also refer to section 3.5, Supporting Information). Following the formation of **6a** under green light, irradiation was stopped, and the reaction manifold was extended by introducing *trans*,*trans*-2,4-hexadien-1-ol (**7**). Without **6a** being formed first, the conjugated diene reacts instantaneously upon mixing with both TAD ends of **6**, slightly favoring addition to the aromatic end (i.e., 53:47, Figure S37). Thus, **6a** formation is essential in ensuring **7** reacts exclusively with the aromatic TAD end to form **7a** (Figure 3c). Once performed, the pink solution of **6a** readily turned colorless upon the addition of **7** (Video S1, Supporting Information), with complete consumption of **6a** into **7a** confirmed via ^{1}H NMR spectroscopy (Figure 3c–d, also refer to Figure S38–40). Finally, the colorless solution containing **7a** was placed in the dark at 25 °C and the cycloreversion was monitored over 24 h by ^{1}H NMR spectroscopy (Table S2 and Figure S41–44). Over the course of this 24 h dark period, an intense pink color formed, owing to the near-quantitative formation of **8** (98 %), with an observed half-life of 5 h (Figure S44–45).

Conclusion

We demonstrate via an in-depth action plot analysis that the absorption spectrum of two very similar 4-substituted TAD moieties does not correlate with their photoreactivity. Specifically, we report on the fascinating example of two substrates that share very similar absorption spectra yet

have vastly different photoreactivity. We show that while the absorption maximum for the aliphatic TAD is at 541 nm, the most efficient wavelength for photoreactivity was 525 nm, which is significantly blue-shifted. In addition, we show that the photoreactivity extends the wavelength region of the broad absorbance band, with efficient photocycloaddition observed between 480 and 580 nm. Most remarkably, we demonstrate that the aromatic TAD substrate shows close to no photoreactivity under the same visible light irradiation, despite having a nearly identical absorption spectrum as its aliphatic TAD counterpart, enabling us to exploit the disparate photoreactivity of both TAD moieties into one single hybrid molecule which displays exceptional photochemical selectivity. This was demonstrated by reversible site-selective photo-modification, allowing for the TAD functionality to be regulated, and for the introduction of a dual-gated reaction manifold. Such a control over photo-reactivity can lead to a facilitated access to synthetically challenging TADs and advance the development of TAD-based light-switchable and dynamic covalent materials.

Acknowledgements

C.B.-K. acknowledges funding from the Australian Research Council (ARC) in the form of a Laureate Fellowship (C.B.-K. FL170100014) enabling his photochemical research as well as continued key support from the Queensland University of Technology (QUT). S.C.G. gratefully acknowledges QUT for a Ph.D. Research Scholarship. C.B.-K. acknowledges key funding by the Deutsche Forschungsgemeinschaft (DFG, German Research Foundation) under Germany's Excellence Strategy for the Excellence Cluster "3D Matter Made to Order" (EXC-2082/1-390761711), by the Carl Zeiss Foundation, and by the Helmholtz program "Materials Systems Engineering". The Central Analytical Research Facility (CARF) at QUT is gratefully acknowledged for access to analytical instrumentation, supported by the Research Portfolio of QUT. H.A.H. acknowledges funding of his EUTOPIA-SIF fellowship received from the European Union's Horizon 2020 research and innovation programme under the Marie Skłodowska-Curie grant agreement No. 945380. H.A.H. thanks the Institute of Advanced Study (IAS) at the University of Warwick for research mobility funding. F.D.P acknowledges the Research Foundation-Flanders (FWO.OPR.2020.0030.01). The authors are grateful to Dr Sarah Walden (University of Jena) for helpful discussions and scientific input regarding the action plot analysis. Additionally, the authors thank Dr Josh Carroll (QUT) for helpful discussions throughout the revision stage. Open Access publishing facilitated by Queensland University of Technology, as part of the Wiley - Queensland University of Technology agreement via the Council of Australian University Librarians.

Conflict of Interest

The authors declare no conflict of interest.

Data Availability Statement

The data that support the findings of this study are available in the Supporting Information of this article. The authors have cited additional references within the Supporting Information.[16,20a,23]

Keywords: Action Plot Analysis · Dynamic Covalent Chemistry · Light-Stabilized Dynamic Materials · Wavelength-Dependent Reactivity

[1] S. Aubert, M. Bezagu, A. C. Spivey, S. Arseniyadis, *Nat. Chem. Rev.* **2019**, *3*, 706–722.
[2] H. Frisch, D. E. Marschner, A. S. Goldmann, C. Barner-Kowollik, *Angew. Chem. Int. Ed.* **2018**, *57*, 2036–2045.
[3] M. M. Lerch, M. J. Hansen, W. A. Velema, W. Szymanski, B. L. Feringa, *Nat. Commun.* **2016**, *7*, 12054–12054.
[4] W. Szymański, J. M. Beierle, H. A. V. Kistemaker, W. A. Velema, B. L. Feringa, *Chem. Rev.* **2013**, *113*, 6114–6178.
[5] a) M. J. Hansen, W. A. Velema, M. M. Lerch, W. Szymanski, B. L. Feringa, *Chem. Soc. Rev.* **2015**, *44*, 3358–3377; b) A. Goulet-Hanssens, F. Eisenreich, S. Hecht, *Adv. Mater.* **2020**, *32*, 1905966.
[6] G. Kaur, P. Johnston, K. Saito, *Polym. Chem.* **2014**, *5*, 2171–2186.
[7] a) M.-M. Russew, S. Hecht, *Adv. Mater.* **2010**, *22*, 3348–3360; b) F. Eisenreich, M. Kathan, A. Dallmann, S. P. Ihrig, T. Schwaar, B. M. Schmidt, S. Hecht, *Nat. Catal.* **2018**, *1*, 516–522; c) M. Kathan, F. Eisenreich, C. Jurissek, A. Dallmann, J. Gurke, S. Hecht, *Nat. Chem.* **2018**, *10*, 1031–1036; d) K. Kuntze, J. Viljakka, M. Virkki, C.-Y. Huang, S. Hecht, A. Priimagi, *Chem. Sci.* **2023**, *14*, 2482–2488.
[8] a) D. N. Barsoum, V. C. Kirinda, B. Kang, J. A. Kalow, *J. Am. Chem. Soc.* **2022**, *144*, 10168–10173; b) R. Dorel, B. L. Feringa, *Chem. Commun.* **2019**, *55*, 6477–6486.
[9] a) N. Armaroli, V. Balzani, J.-P. Collin, P. Gaviña, J.-P. Sauvage, B. Ventura, *J. Am. Chem. Soc.* **1999**, *121*, 4397–4408; b) B. L. Feringa, N. Koumura, R. W. J. Zijlstra, R. A. van Delden, N. Harada, *Nature* **1999**, *401*, 152–155; c) K. Grill, H. Dube, *J. Am. Chem. Soc.* **2020**, *142*, 19300–19307.
[10] I. M. Irshadeen, S. L. Walden, M. Wegener, V. X. Truong, H. Frisch, J. P. Blinco, C. Barner-Kowollik, *J. Am. Chem. Soc.* **2021**, *143*, 21113–21126.
[11] E. Skolia, C. G. Kokotos, *ACS Org. Inorg. Au* **2023**, *3*, 96–103.
[12] O. P. Demchuk, O. V. Hryshchuk, B. V. Vashchenko, A. V. Kozytskiy, A. V. Tymtsunik, I. V. Komarov, O. O. Grygorenko, *J. Org. Chem.* **2020**, *85*, 5927–5940.
[13] a) I. M. Irshadeen, K. De Bruycker, A. S. Micallef, S. L. Walden, H. Frisch, C. Barner-Kowollik, *Polym. Chem.* **2021**, *12*, 4903–4909; b) P. W. Kamm, J. P. Blinco, A.-N. Unterreiner, C. Barner-Kowollik, *Chem. Commun.* **2021**, *57*, 3991–3994; c) D. E. Fast, A. Lauer, J. P. Menzel, A.-M. Kelterer, G. Gescheidt, C. Barner-Kowollik, *Macromolecules* **2017**, *50*, 1815–1823; d) D. E. Marschner, P. W. Kamm, H. Frisch, A.-N. Unterreiner, C. Barner-Kowollik, *Chem. Commun.* **2020**, *56*, 14043–14046; e) S. Bialas, L. Michalek, D. E. Marschner, T. Krappitz, M. Wegener, J. Blinco, E. Blasco, H. Frisch, C. Barner-Kowollik, *Adv. Mater.* **2019**, *31*, 1807288; f) K. Kalayci,

H. Frisch, V. X. Truong, C. Barner-Kowollik, *Nat. Commun.* **2020**, *11*, 4193–4193.
[14] N. J. Turro, A. A. Lamola, in *The Science of Photobiology* (Ed.: K. C. Smith), Springer US, Boston, MA, **1977**, pp. 63–86.
[15] H. Frisch, F. R. Bloesser, C. Barner-Kowollik, *Angew. Chem. Int. Ed.* **2019**, *58*, 3604–3609.
[16] H. A. Houck, E. Blasco, F. E. Du Prez, C. Barner-Kowollik, *J. Am. Chem. Soc.* **2019**, *141*, 12329–12337.
[17] a) D. Kodura, H. A. Houck, F. R. Bloesser, A. S. Goldmann, F. E. Du Prez, H. Frisch, C. Barner-Kowollik, *Chem. Sci.* **2021**, *12*, 1302–1310; b) E. Liarou, H. A. Houck, F. E. Du Prez, *J. Am. Chem. Soc.* **2022**, *144*, 6954–6963.
[18] a) C. W. Schmitt, S. L. Walden, L. Delafresnaye, H. A. Houck, L. Barner, C. Barner-Kowollik, *Polym. Chem.* **2021**, *12*, 449–457; b) S. C. Gauci, M. Gernhardt, H. Frisch, H. A. Houck, J. P. Blinco, E. Blasco, B. T. Tuten, C. Barner-Kowollik, *Adv. Funct. Mater.* **2023**, 2206303; c) A. J. Ghielmetti, C. Barner-Kowollik, F. E. Du Prez, H. A. Houck, *Polym. Chem.* **2023**, *14*, 1554–1566; d) S. C. Gauci, K. Ehrmann, M. Gernhardt, B. Tuten, E. Blasco, H. Frisch, V. Jayalatharachchi, J. P. Blinco, H. A. Houck, C. Barner-Kowollik, *Adv. Mater.* **2023**, *35*, e2300151.
[19] a) H. Wamhoff, K. Wald, *Chem. Ber.* **1977**, *110*, 1699–1715; b) F. Risi, A.-M. Alstanei, E. Volanschi, M. Carles, L. Pizzala, J.-P. Aycard, *Eur. J. Org. Chem.* **2000**, 617–626; c) B. Golba, M. Soete, Z. Zhong, N. Sanders, F. E. Du Prez, H. A. Houck, B. G. De Geest, *Angew. Chem. Int. Ed.* **2023**, *62*, e202301102; d) H. A. Houck, P. Müller, M. Wegener, C. Barner-Kowollik, F. E. Du Prez, E. Blasco, *Adv. Mater.* **2020**, *32*, 2003060.
[20] a) D. P. Kjell, R. S. Sheridan, *J. Am. Chem. Soc.* **1984**, *106*, 5368–5370; b) G. W. Breton, K. A. Newton, *J. Org. Chem.* **2000**, *65*, 2863–2869.
[21] W. H. Pirkle, J. C. Stickler, *J. Am. Chem. Soc.* **1970**, *92*, 7497–7499.
[22] a) H. A. Houck, K. De Bruycker, C. Barner-Kowollik, J. M. Winne, F. E. Du Prez, *Macromolecules* **2018**, *51*, 3156–3164; b) A. G. Leach, K. N. Houk, *Chem. Commun.* **2002**, 1243–1255; c) R. C. Cookson, S. S. H. Gilani, I. D. R. Stevens, *Tetrahedron Lett.* **1962**, *3*, 615–618; d) W. H. Pirkle, J. C. Stickler, *Chem. Commun.* **1967**, 760; e) K. De Bruycker, S. Billiet, H. A. Houck, S. Chattopadhyay, J. M. Winne, F. E. Du Prez, *Chem. Rev.* **2016**, *116*, 3919–3974.
[23] a) J. P. Menzel, B. B. Noble, A. Lauer, M. L. Coote, J. P. Blinco, C. Barner-Kowollik, *J. Am. Chem. Soc.* **2017**, *139*, 15812–15820; b) S. Billiet, K. De Bruycker, F. Driessen, H. Goossens, V. Van Speybroeck, J. M. Winne, F. E. Du Prez, *Nat. Chem.* **2014**, *6*, 815–821; c) O. Türünç, S. Billiet, K. De Bruycker, S. Ouardad, J. Winne, F. E. Du Prez, *Eur. Polym. J.* **2015**, *65*, 286–297; d) U. Burger, Y. Mentha, P. Jean Thorel, *Helv. Chim. Acta* **1986**, *69*, 670–675; e) E. H. Southgate, J. Pospech, J. Fu, D. R. Holycross, D. Sarlah, *Nat. Chem.* **2016**, *8*, 922–928.

Manuscript received: July 19, 2023
Accepted manuscript online: August 8, 2023
Version of record online: ■■, ■■

Research Articles

Photochemistry

S. C. Gauci, F. E. Du Prez, J. O. Holloway, H. A. Houck,* C. Barner-Kowollik* _____ **e202310274**

The Power of Action Plots: Unveiling Reaction Selectivity of Light-Stabilized Dynamic Covalent Chemistry

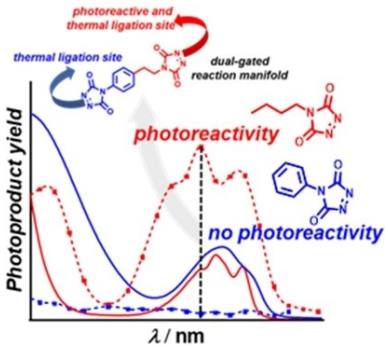

The power of action plots is demonstrated by unveiling a reaction selective window between two different substituted triazolinediones that exhibit near identical absorbance spectra. The remarkable difference in photoreactivity is exploited by designing a dual-gated reaction manifold, which demonstrates the site-selective (photo)chemical behavior of both triazolinedione substrates within a single small molecule.